

THE CLASSIFICATION OF INTRINSIC VARIABLES. V. THE LARGE-AMPLITUDE RED VARIABLES

O. J. EGGEN

Mount Stromlo and Siding Spring Observatory, Research School of Physical Sciences,
 The Australian National University

Received 1974 June 27

ABSTRACT

(*UBVRI*) observations covering several cycles of 10 large-amplitude red field variables and three probable group members are discussed. The individual observations are published separately in a supplement. Although large variations occur between cycles on the rising branches and at maxima in the light curves, the curves for different cycles coalesce on the descending branch from phase 0.25 to near minimum light. Median values of the magnitude in all colors, obtained from light curves in intensity units, are closely approximated by observed values at phase 0.25. When the giant sequence in the ($M_{\text{bol}}, R - I$)-plane, obtained from constant stars, is extended to higher luminosities through the use of median magnitudes of small- and intermediate-variables, the large-amplitude variables lie near this sequence at phase 0.25. The median luminosities are closely approximated by the color-luminosity relation $\langle M_{\text{bol}} \rangle = -0.65 \text{ mag} - 2.5 \langle (R - I)_0 \rangle$, where $\langle (R - I)_0 \rangle$ is used at phase 0.25. Because the periods and median colors are well correlated for the large-amplitude variables, $\langle (R - I)_0 \rangle = -0.45 \text{ mag} + 0.90 \log P$, the color-luminosity relation is also a period-luminosity relation, $\langle M_{\text{bol}} \rangle = +0.5 \text{ mag} - 2.25 \log P$. However, the well determined bolometric corrections for stars with periods between 100 and 500 days are closely correlated with color, $\text{B.C.} = +0.60 \text{ mag} - 2.5(R - I)$, so no period-luminosity relation is expected in the visual luminosities over this range of period, $\langle M_V \rangle = -1.25 \text{ mag}$.

Subject headings: late-type stars — long-period variables — photometry — variable stars

I. INTRODUCTION

The present paper in this series is concerned with the red variables of visual amplitudes greater than 2 mag and with relatively stable periods and light curves. Many, but not all, of these stars have been called "Mira variables," although this term, the meaning of which has changed over the years, can be misleading in some instances. In the present context they will be called large-amplitude red variables.

Although these stars are usually recognized as the most stable of the red variables, their light curves and periods are probably even more stable than generally believed. Visual observations, by the members of the Royal Astronomical Society of New Zealand, covering four consecutive cycles of the large-amplitude red variable R Car are shown in figure 1 where the open circles represent mean magnitudes obtained on the dates given in the figure; the crosses, those advanced one period (310^d) from the date of observations; and the

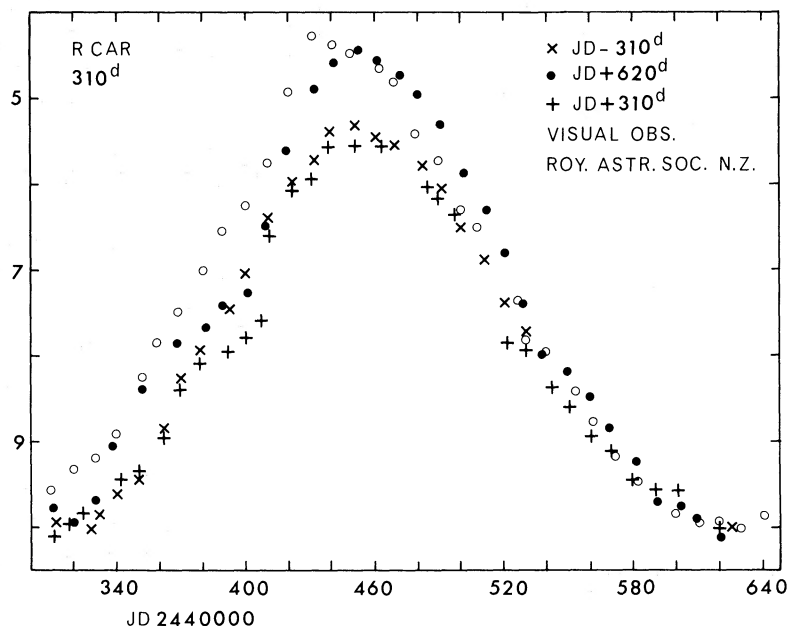


FIG. 1.—Light curves for R Car from visual observations

plus signs and filled circles, those folded back one and two periods, respectively. Some concurrent photoelectric observations confirm the high accuracy of these visual results and give $V_E = \text{Vis.}(NZ) - 0.2$ mag. A period of 310 days was found for R Car soon after its discovery 100 years ago, but a large body of literature for this and similar stars has been built up on the subject of small period variations which, in the present case, range from about 306 to 314 days, with some of the changes occurring from cycle to cycle. Many of these periods have been determined from observations made near maximum light; indeed, an apparently variable period could be inferred from the maxima shown in figure 1, although only four cycles are involved. However, the main deviations from cycle to cycle in figure 1 are on the rising branch and near maximum light whereas the descending branch of the light curve, especially about 70 to 150 days after maximum, is little changed. It is a reasonable assumption that the variations both in epoch and in luminosity of maximum are connected with the appearance of, and changes in, the emission lines in the spectra near maximum, but more simultaneous photometric and spectroscopic investigations are necessary to confirm and detail the physical basis of this connection (e.g., Lockwood and Wing 1971).

The apparent variation in the light curves, at some phases, between different cycles will be discussed below in greater detail for individual stars with the view of finding a phase or series of phases at which photometric parameters characteristic of the variable might be obtained and substituted for entire light curves. The most obvious parameters are those involving the median values of, say, V_E , $B - V$, $V - R$, and $R - I$, but these are not only costly to obtain in terms of observing time, but are also difficult to interpret because of possible large variations with phase in the band and line blocking over the bandpasses of the filters used in the photometry.

$UBVRI$ observations over several cycles have been obtained in the last 5 years for about 50 large-amplitude red variables, and the following sections contain a discussion of some of the most completely observed light curves and a calibration of the luminosities based on the few members of stellar groups and clusters.

The following transformations used here are discussed in detail elsewhere:

$$R = R_J + 0.38 \quad (J = \text{Johnson } 1966),$$

$$(R - I) = 0.8(R - I)_J - 0.05 \text{ mag} \quad (\text{Eggen } 1971c),$$

$$M_{\text{bol}} = M(I)_J + 1 \text{ mag} \quad (\text{Eggen } 1971a),$$

$$E'(B - V) = E(B - V) \text{ at } B - V = 0,$$

$$E(B - V) = 0.8E'(B - V) \text{ at } B - V = +1.5$$

$$(\text{Eggen } 1974a; \text{Ferne } 1963),$$

$$E(R - I) = 0.7E(B - V) \quad (\text{Eggen } 1969b).$$

Most of the observations discussed here are represented in light and color curves. The individual obser-

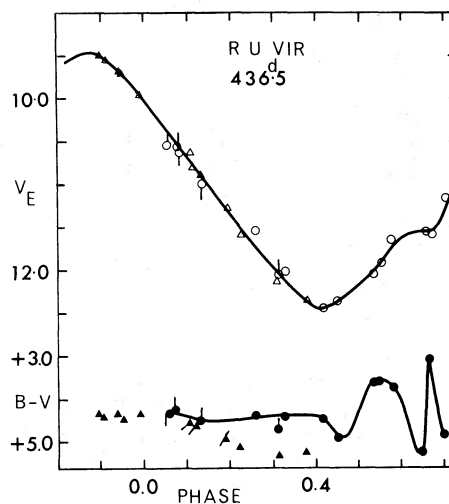


FIG. 2.—Light and color curves (VB) for RU Vir

variations are published separately in an *Ap. J. Supplement* (Eggen 1974b, referred to here as SUPP).

II. INDIVIDUAL FIELD VARIABLES

The stars are discussed in order to decreasing period. In general, the observations in different cycles are shown on the light curves as different symbols, with open symbols used for magnitudes and filled symbols for colors.

a) RU Virginis

The observations of this carbon star are in figures 2 and 3. The circles represent consecutive cycles, with flags designating the later cycle. The maximum was covered only in the third cycle (triangles), but the light curves in all three cycles coalesce on the descending branch. The standstill or ledge on the rising branch is typical of light curves for carbon stars, as is the lack of appreciable variation in $R - I$.

b) R Octantis

The observations are in figures 4 and 5. Two, successive cycles were observed with triangles representing

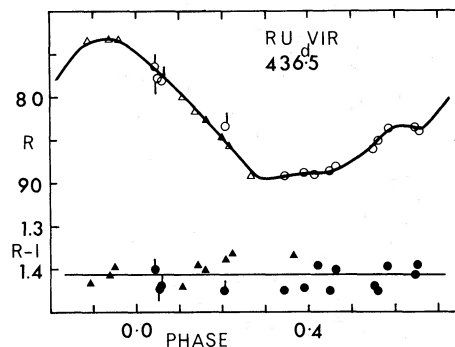
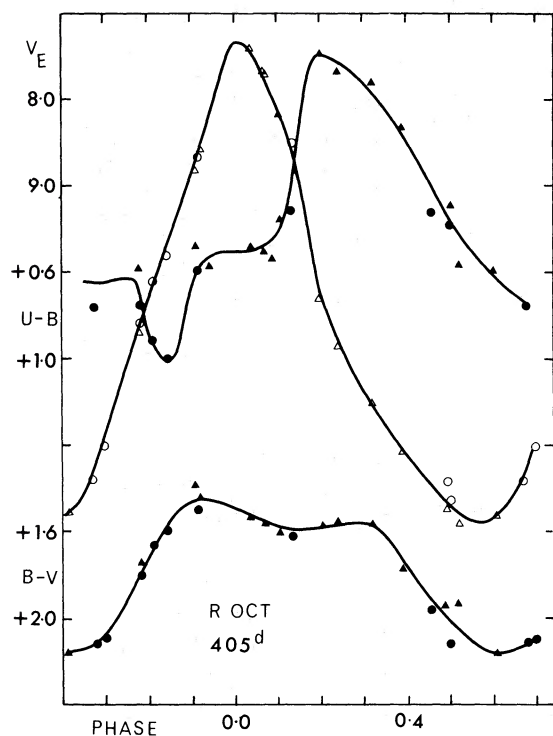


FIG. 3.—Same as fig. 2 but for (RI)

FIG. 4.—Light and color curves (*UBV*) for R Oct

the latter cycle in the figures. Visual observations have indicated a range of nearly 2 mag in the luminosity at maximum, but the present cycles represent the average maxima.

c) *RR Sagittarii*

Observations covering three consecutive maxima and descending branches are shown in figure 6. The separation noted in figure 6 (and fig. 1) of maximum light in the light curves of different cycles becomes less noticeable in the *R* and especially the *I* observations.

d) *R Carinae*

The observations covering three separate cycles are shown in figure 7. The minimum observed in 1970

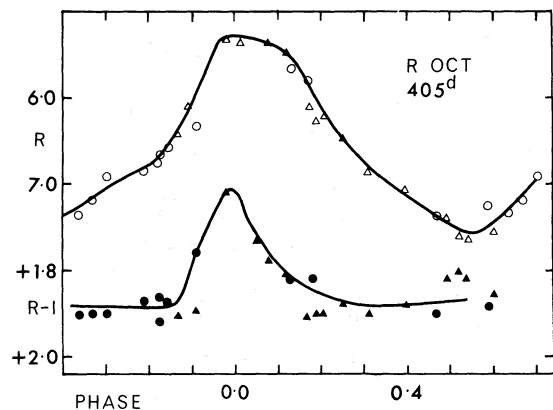
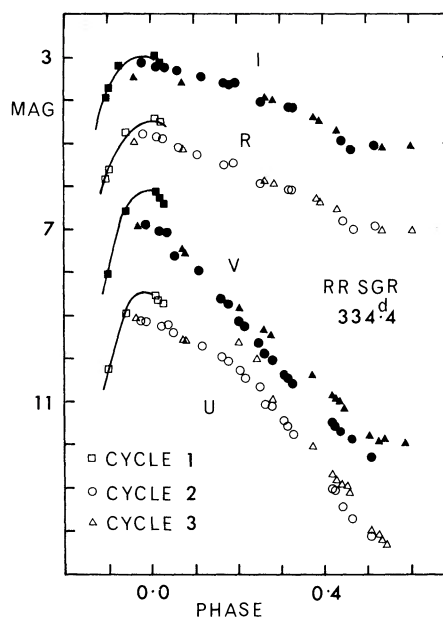
FIG. 5.—Same as fig. 4 but for (*RI*)

FIG. 6.—Light curves for RR Sgr

agrees well with that from the visual observations in figure 1, but the maxima observed have all been less extreme than those represented in that figure. However, figures 1 and 7 can be related through the visual observations in 1970, represented by crosses in both figures, and these show that the maximum reached just after the last photoelectric observations in that year was one of the faintest in figure 1. These visual observations were taken from Royal Astronomical Society of New Zealand Circular No. 168 and were corrected by -0.20 mag before plotting in figure 7.

e) *T Columbae*

These observations, covering two cycles, are shown in figures 8 and 9. The period of $225^d.52$ is based on over 50 years of visual observations which, like those for R Car, indicate a small variation of period in the range of 5 or 6 days. The two observed maxima are separated by two cycles, and, like the two similarly separated maxima of R Carinae indicated in figure 1 by open and filled circles, the luminosity at maximum is the same but the rise to that luminosity in *U*, *B*, and *V* is considerably depressed in one cycle. A discontinuity near phase 0.9 in the light curves represented by circles in figure 8 is apparent in all three colors and is especially prominent in the *R* and *I* curves of figure 9. It is notable that except for this discontinuity, the light curves in *I* are essentially the same in the two cycles. The cycle represented by circles in figures 8 and 9 gives the median values, after converting to intensity units, of $\langle U \rangle = 10.74$ mag, $\langle B \rangle = 9.84$ mag, $\langle V \rangle = 8.35$ mag, $\langle R \rangle = 6.32$ mag, and $\langle I \rangle = 4.83$ mag. These medians correspond closely to the observed values near phase 0.25 after maximum light. This is the phase (e.g., fig. 1) where the light curves from different cycles begin to coalesce.

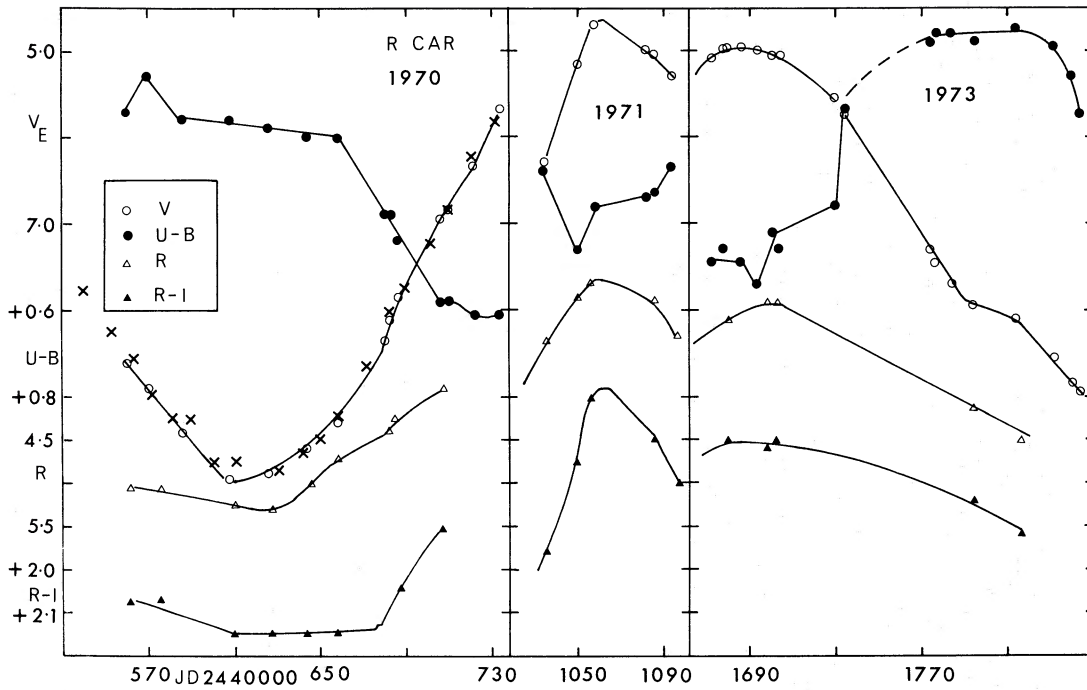


FIG. 7.—Light and color curves for R Car

f) *T Horologii*

Observations made in four cycles are folded on a period of 217 days in figures 10 and 11. The distortion at maximum visual light, from cycle to cycle, is very marked and could explain the range of periods suggested for this star. Typically, this distortion nearly

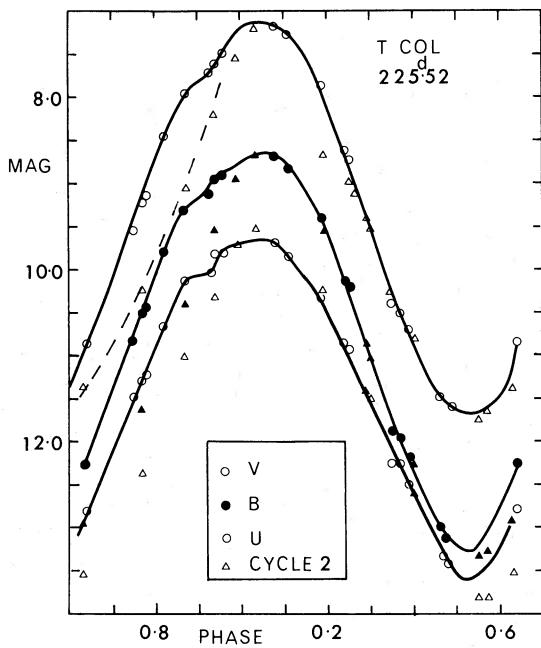


FIG. 8.—Light curves (UBV) for T Col

disappears in *I*, and the light curves in *V* coalesce at quarter phase on the descending branch.

g) *R Virginis*

The observations made in 1971, 1972, and 1973 are shown in figure 12. Earlier observations (Eggen 1967) made in 1966 and by Barnes (1974) in 1969 and 1970 are shown in figure 13. The light curves, especially on the ascending branches, show a large range of shapes, but again the descending branches, after phase 0.25, coalesce. The range in *R - I*, from +0.8 mag to +2.2 mag, is the largest observed. This star was previously considered a possible candidate for membership in the Hyades Group (Eggen 1972d) on the basis of its blue color at maximum, but, as discussed below, its space velocity is much higher from its

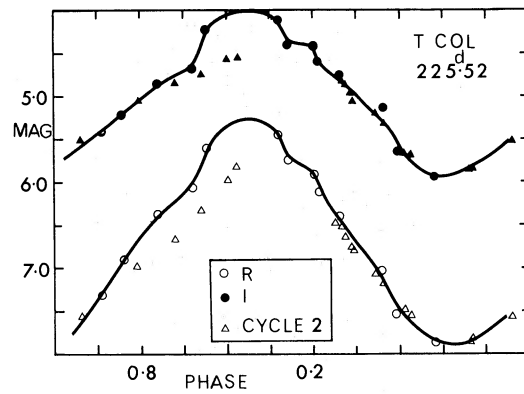
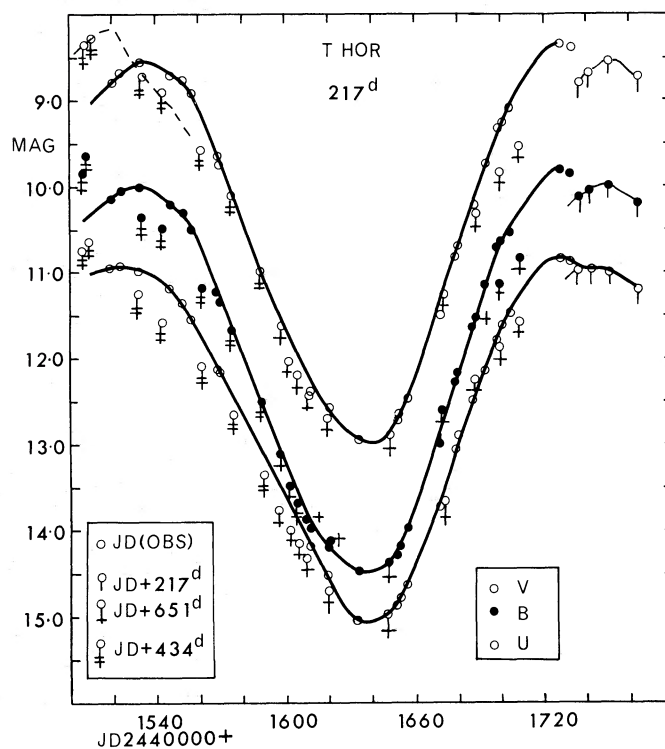


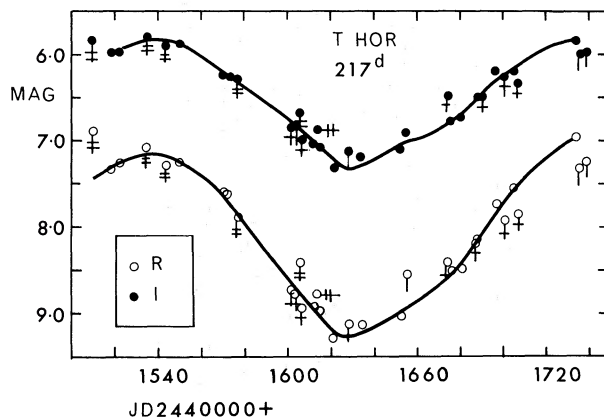
FIG. 9.—Same as fig. 8 but for (RI)

FIG. 10.—Light curves (*UBV*) for T Hor

median color and the calibration of luminosities derived here.

h) T Gruis and R Vulpeculae

These stars with nearly identical periods will be discussed together. The observations of T Gru are in figures 14 and 15. The circles in the figures represent a long run covering two maxima in 1970, and the flagged symbols represent the second of these maxima, which was nearly a magnitude fainter in *V* than the first. The observations of R Vul are shown in figure 16. The observations of this variable are fewer but the

FIG. 11.—Same as fig. 10 but for (*RI*)

light curves are well defined; and although they show a considerably larger amplitude than those for T Gru, this may only be an accident, resulting from the limitations of the observations to one maximum. Some observations by Barnes (1974) covering three cycles are shown as crosses in figure 16, except one maximum which is shown as a plus sign. As for the other variables discussed here, maximum light varies from cycle to cycle, but this variation disappears on the descending branch of the light curves.

i) W Puppis

The shortest periods known for large-amplitude red variables are about 110 or 120 days. One of the shortest is that for W Pup (120^d). The observed light curves in *I*, *R*, *V_E*, and *U*, which cover four of five consecutive cycles, are shown in figure 17 where the variations from cycle to cycle on the rising branch are evident.

III. LARGE-AMPLITUDE VARIABLES IN GROUPS AND CLUSTERS

a) Hyades Group

The giant sequence for group stars redder than $R - I = +0.6$ mag is shown in figure 18. The section from $R - I = +0.6$ to $+0.8$ mag is from the nonvariable stars in the group (Eggen 1974a, table 3), and the extension to $R - I = +1.6$ mag is estimated from the mean luminosities and colors of the small amplitude variables (e.g., Eggen 1973a, table 9). The individual

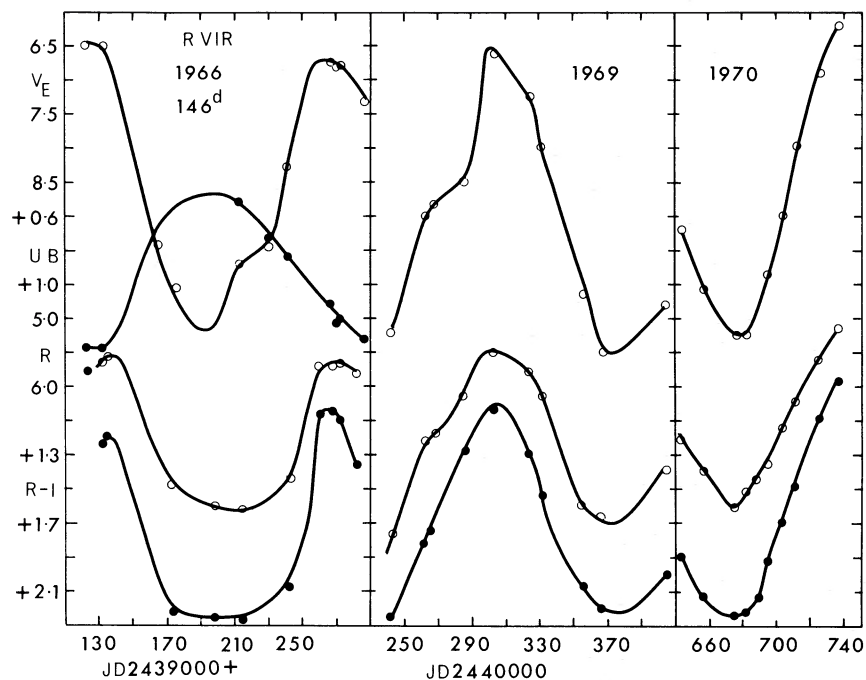


FIG. 12.—Light and color curves for R Vir

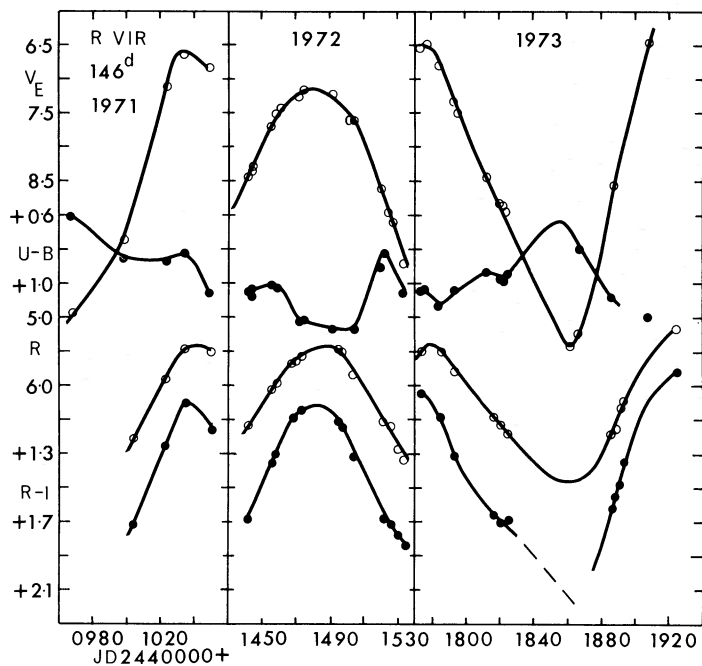
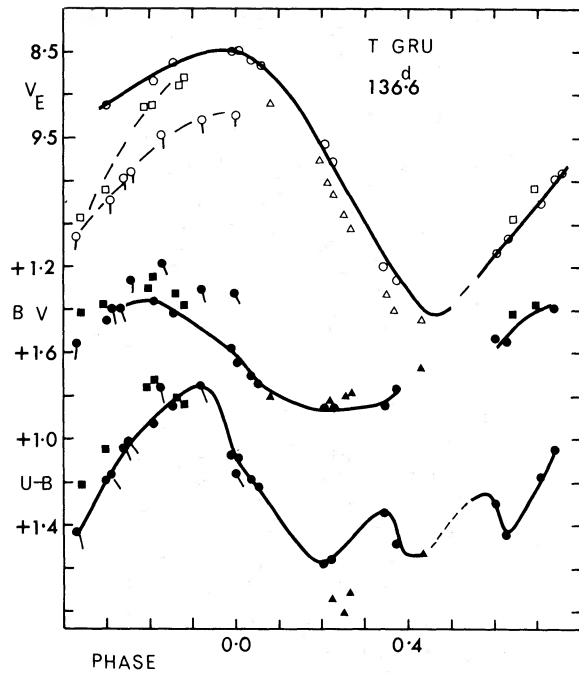


FIG. 13.—Same as fig. 12

FIG. 14.—Light and color curves (*UBV*) for T Gru

small-amplitude variables, all with visual amplitudes of 0.5 mag or less, are listed elsewhere (Eggen 1973*b*, table 3) and are shown as filled circles in figure 18. An additional, redder group star, which belongs to the class of intermediate (i.e., visual amplitude of 0.5–2.0 mag) amplitude variables that will be discussed elsewhere, is π^1 Gruis. All the observations are shown in figure 19. Like most of the intermediate-amplitude red variables, the light variation is only quasi-periodic and the light curve in the basic period, which in the present case is near 150 days, is modulated in a secondary period that is an order of magnitude longer.

The proper motion of π^1 Gruis is accurately known from meridian observations; and on the FK4 system,

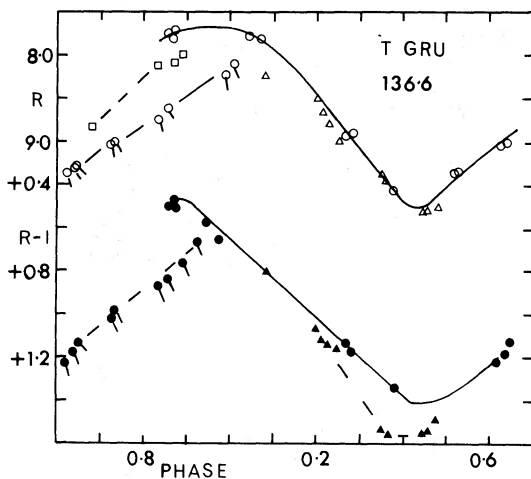
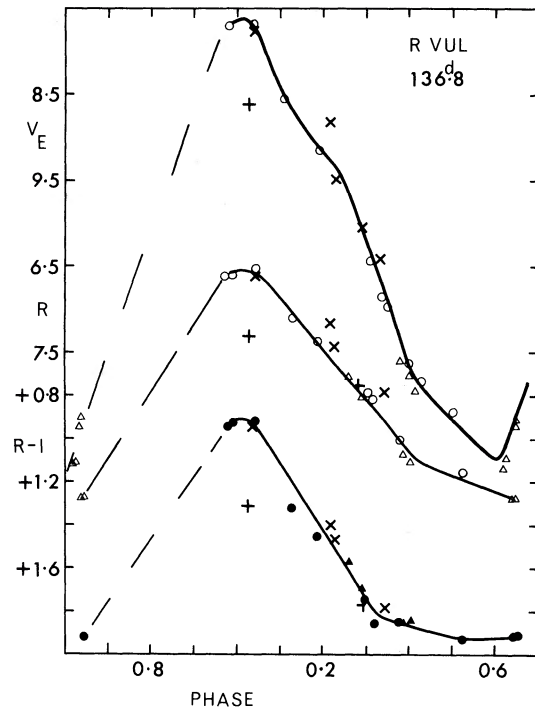
FIG. 15.—Same as fig. 14 but for (*RI*)

FIG. 16.—Light and color curves for R Vul

with precessional corrections, the values are $(\mu_\alpha, \mu_\delta) = (+0^{\circ}031, -0^{\circ}013)$. The radial velocity is -19.6 km s^{-1} and, as a member of the Hyades Group, $(U, V, W) = (+35, -16.8, +2) \text{ km s}^{-1}$ (e.g., Eggen 1974*a*) with a modulus of 6.6 mag. The star has a galactic latitude of -55° , so the reddening is probably very small. The group modulus has been used to trace the mean variation shown by boxes in the $(M_{\text{bol}}, R - I)$ -plane of figure 18.

As discussed elsewhere (Eggen 1971*b*), the long-period (392^d) variable R Hya is also a member of the Hyades Group. The phases have been computed from the elements $\text{Max.} = \text{JD } 2,441,676 + 392^{\text{d}}0E$. The period appears to be decreasing at the rate of nearly 50 days a century (see references in the *General Catalog of Variable Stars* [GCVS]). The observations were made in four cycles which are distinguished by different symbols in figures 20 and 21, and some observations obtained in 1964 by Mendoza (1967) are indicated by crosses. The proper motion of the variable is well determined from meridian observations, and on the FK4 system with precessional corrections it is $(\mu_\alpha, \mu_\delta) = (-0^{\circ}056, +0^{\circ}014)$ with a probable error near $0^{\circ}002$. The radial velocity is -6.0 km s^{-1} , and membership in the Hyades Group gives $(U, V, W) = (+41, -16.8, +11) \text{ km s}^{-1}$ with a modulus of 6.1 mag. This modulus is identical to that obtained from the common-proper-motion companion (Eggen 1971*b*). The variable has a galactic latitude of $+39^\circ$, so the previously adopted reddening (Eggen 1971*b*) of $E'(B - V) = +0.03 \text{ mag}$ appears reasonable, and from Fernie's precepts (e.g., Eggen 1974*a*), $E(B - V)$

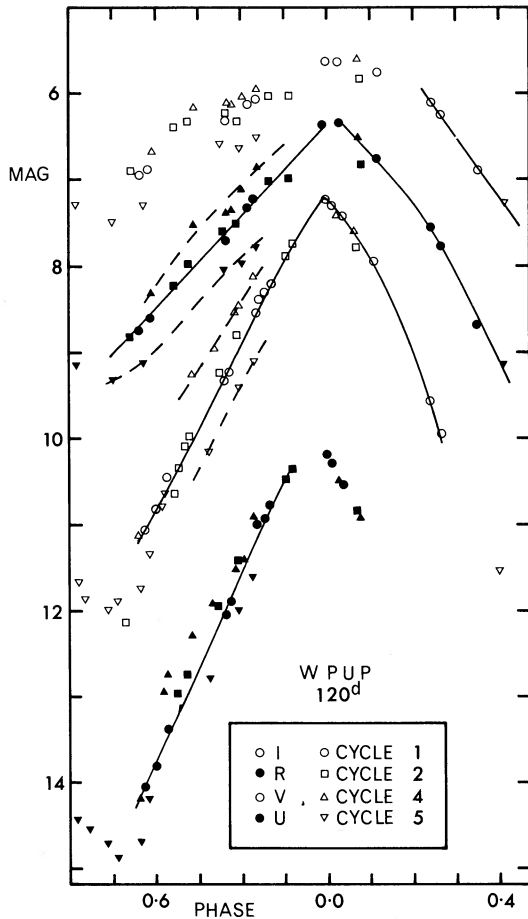


FIG. 17.—Light curves for W Pup

at $B - V = +1.5$ mag is then only 0.02 mag with $E(R - I) = 0.015$ mag. This small reddening will be ignored. The path traced by the variable in the $(M_{bol}, R - I)$ -plane is shown in figure 18 by open circles, and the mean light and color curves are tabulated in table 1.

Another probable member of the Hyades Group is the large-amplitude red variable RR Sco. The observations in two consecutive cycles are shown with different symbols in figures 22 and 23 where the

elements used are $Max. = JD\ 2,441,476 + 280.0E$. The proper motion of RR Sco, derived from meridian observations, is $(\mu_{\alpha}, \mu_{\delta}) = (-0.010, -0.013)$ on the FK4 system with precessional corrections. Unfortunately this motion is not as well established as that for π^1 Gru and R Hya, but two photographic determinations (Hoffleit 1967; Alden and Osvalds 1961) give an almost identical mean, $(-0.009, -0.014)$ on the same system. The radial velocity is $-36.0\ km\ s^{-1}$, and membership in the Hyades Group gives $(U, V, W) = (+38, -16.8, -5)\ km\ s^{-1}$ with a modulus of 7.2 mag. The reddening of $E(B - V) = +0.12$ mag is interpolated in table 2 which also contains reddening determinations for the field variables discussed in the previous section. The observations of the B-type stars in table 2 are by the Cape observers (C), or are based on new results and designated by the number of observations with the 40-inch (1-m) reflector.

The mean light and color curves for RR Sco are tabulated in table 1 and are shown as open circles in figure 18. The broken extension to the Hyades $(M_{bol}, R - I)$ -relation in figure 18 is a linear extrapolation of the continuous curve and would satisfactorily yield mean luminosities for the three variables discussed here if we adopt the median of the observed parameters of the intermediate-amplitude variable π^1 Gru and the $(R, R - I)$ values at phases 0.2–0.3 for the large-amplitude variables. In the preceding section it was found that the median values of $UBVRI$ obtained from complete light curves, converted to intensity units, closely approximate those read at phase 0.25 after maximum light, where the light curves in various cycles coalesce. For the V and R curves of R Hya tabulated in table 1 the values of $\langle V \rangle = 7.4$ mag and $\langle R \rangle = 4.8$ mag, which correspond to phases 0.23 and 0.275, respectively.

b) Old Disk Population Groups and Clusters

The giant sequence from the old disk groups and clusters (Eggen 1973a, table 9) is shown as a continuous curve in figure 24. The Hyades sequence, from figure 18, is shown as a broken curve to $R - I$ near +1.1 mag where the sequences join. The small-amplitude variables in the ζ Her, Wolf 630, and 61 Cyg groups (Eggen 1973b, table 1) and FG Vul in NGC 6940 (Eggen 1973b fig. 17), upon which the sequence in figure 24 redder

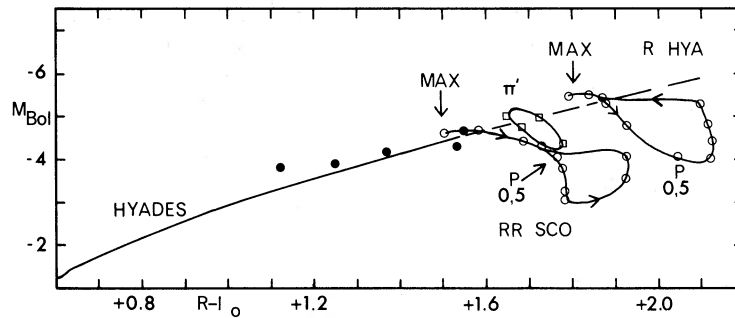


FIG. 18.—The Hyades Group variables in the $(M_{bol}, R - I)$ -plane

TABLE 1
 MEAN LIGHT CURVES

Phase	V_E	B-V	U-B	R	R-I	M_{bol}	Phase	V_E	B-V	U-B	R	R-I	M_{bol}
R HYA $E(R-I) = 0.00$ mag													
0.00	4.8		+0.75	2.25	+1.79	-5.5	0.50	8.8		+0.37	4.15	+2.12	-4.0
0.10	5.4		+0.55	2.3	+1.83	-5.55	0.60	8.45		+0.48	4.0	+2.12	-4.2
0.20	6.4		+0.50	2.55	+1.88	-5.35	0.70	7.25		+0.52	3.3	+2.12	-4.9
0.30	7.4		+0.45	3.15	+1.94	-4.8	0.80	5.5		+0.5	2.75	+2.00	-5.3
0.40	8.4		+0.37	4.0	+2.05	-4.1	0.90	5.0		+0.5	2.4	+1.87	-5.5
RR SCO $E(R-I) = +0.07$ mag													
0.00	6.1	+1.50	+0.8	4.15	+1.57	-4.55	0.50	10.35	+1.70	-	5.8	+1.85	-3.2
0.10	6.25	+1.57	+0.65	4.2	+1.65	-4.6	0.60	10.5	+1.64	+0.5	6.0	+1.85	-3.05
0.20	7.0	+1.55	+0.45	4.5	+1.76	-4.45	0.70	10.0	+1.60	+0.5	5.8	+2.00	-3.45
0.30	8.2	+1.57	+0.25	4.9	+1.85	-4.15	0.80	8.45	+1.45	+0.75	5.2	+2.00	-4.0
47 TUC No. 3 $E(R-I) = +0.02$ mag													
0.00	10.0	+1.62	+1.05	9.2	+0.73	-4.6	0.50	15.25	+1.22	+0.5	12.2	+2.00	-3.15
0.10	11.1	+1.56	+1.16	9.6	+1.10	-4.65	0.60	14.95	+1.20	+0.5	11.95	+1.93	-3.35
0.20	12.15	+1.62	+1.00	10.2	+1.38	-4.4	0.70	13.1	+1.24	+0.8	11.05	+1.74	-4.0
0.30	13.25	+1.41	+0.98	11.1	+1.72	-3.8	0.80	12.05	+1.24	+0.8	10.35	+1.44	-4.2
0.40	14.50	+1.27	+1.0	11.85	+1.90	-3.4	0.90	10.9	+1.32	+0.8	9.65	+0.96	-4.4

than $R - I = +1.0$ mag is based, are shown as filled circles at median luminosity; all of these variables have visual amplitudes less than 0.5 mag.

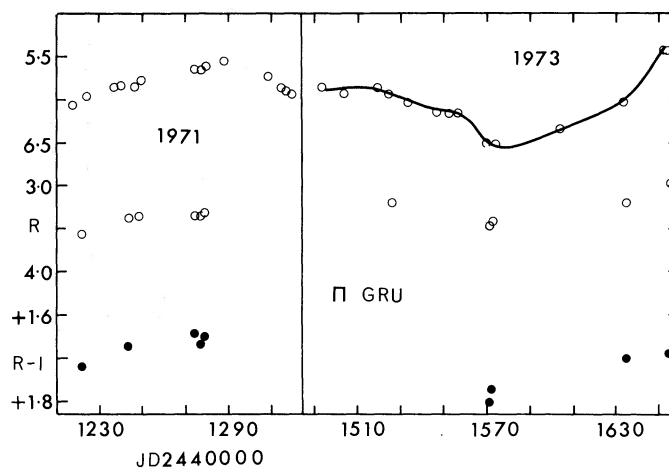
Three additional stars, all typical of the intermediate-amplitude variables, are also group members: SW Vir (61 Cyg Group), S Lep (Wolf 630 Group), and θ Aps (ζ Her Group).

The available observations of SW Vir are shown in figure 25. As already noted, the characteristics of the intermediate-amplitude variables are the quasi-periodicity, which in the present case is near 150 days, and the modulation of the light curves in a secondary period that is about an order of magnitude longer. The proper motion derived from meridian observations is well determined (Blackwell and Lowne 1968), and on the FK4 system with precessional corrections it is $(\mu_\alpha, \mu_\delta) = (-0''.065, -0''.004)$ with a probable error near $0''.003$. The radial velocity is -15.0 km s $^{-1}$, and,

as a member of the 61 Cyg Group, $(U, V, W) = (+73, -53, -8)$ km s with a modulus of 7.4 mag. The path traced in the $(M_{bol}, R - I)$ -plane during the 1970 cycle shown in figure 25 is indicated by boxes in figure 24.

The light and color curves of S Lep are shown in figure 26. The basic and secondary periods are near 90 and 900 days, respectively (see GCVS). An earlier estimate of the reddening gave $E(B - V) = +0.05$ mag (Eggen 1971*b*) or $E(R - I) = +0.03$ mag, and this value is used here. The well-determined proper motion (Blackwell and Lowne 1968) on the FK4 system with precessional corrections is $(\mu_\alpha, \mu_\delta) = (+0''.012, -0''.015)$ with a probable error near $0''.003$, and the radial velocity is $+12.0$ km s $^{-1}$. Membership in the Wolf 630 Group gives

$$(U, V, W) = (-16, -33, +10) \text{ km s}^{-1}$$


 FIG. 19.—Light and color curves for π^1 Gru

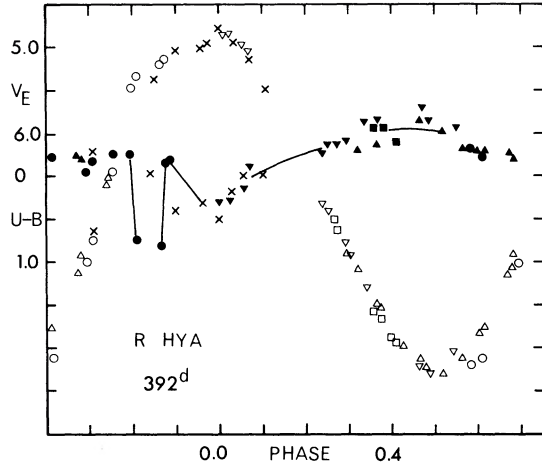
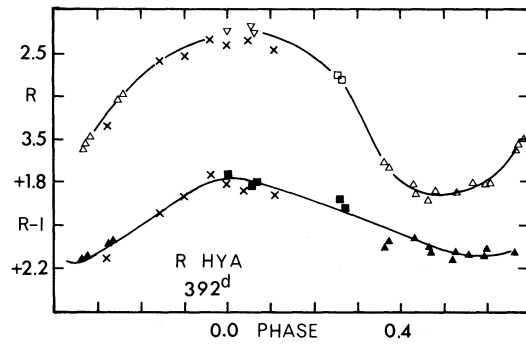
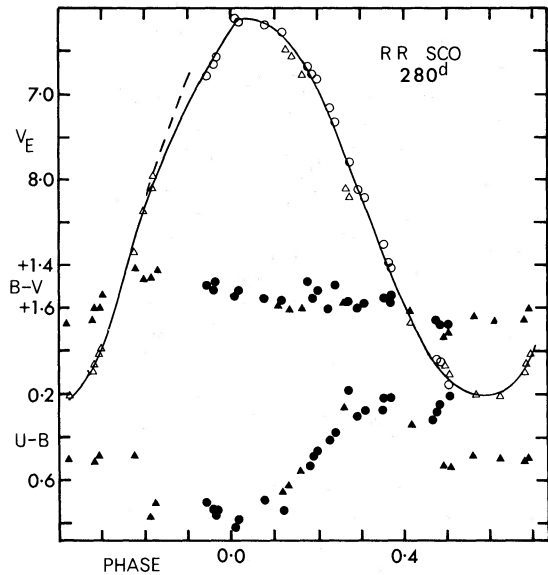
FIG. 20.—Light and color curves (*UBV*) for R HyaFIG. 21.—Same as fig. 20 but for (*RI*)

TABLE 2

REDDENING DETERMINATIONS

Name	l	b	V_E (mag)	$B-V$ (mag)	$U-B$ (mag)	S	Sp	E'	R (ps)
R Car	282.3	- 8.2						+0.07	260
HD 79351	277.7	- 7.4	3.44	-0.19	-0.70	C	B3IV	+0.02	210
79447	280.0	- 9.6	3.97	-0.18	-0.67	C	B3III	+0.02	295
82764	278.0	- 4.0	7.14	+0.01	-0.335	2	B8	+0.155	375
82790	285.0	-11.0	8.80	+0.05	-0.255	2	B9		
82834	281.0	- 7.3	7.12	+0.10	-0.045	2	A0	+0.17	150
82919	278.0	- 4.0	7.15	-0.03	-0.495	2	B5	+0.15	330
83944	281.9	- 6.6	4.51	-0.07	-0.20	C	B9V	+0.02	65
83945	282.0	- 7.0	7.62	-0.01	-0.30	C	B8	+0.13	320
R Vul*	70.5	-15.2						+0.15	590
W Pup	256.2	- 8.7						+0.15	1300
HD 62804	255.3	- 9.0	8.88	+0.03	-0.145	2	B9	+0.12	365
63118	257.5	- 9.5	6.03	-0.07	-0.40	2	B6	+0.08	180
63308	254.4	- 7.5	6.58	-0.09	-0.675	2	B3V	+0.13	350
63425	255.2	- 8.5	6.95	-0.16	-0.935	2	B2	+0.13:	500:
63578	260.0	-10.5	5.22	-0.84	-0.84	C	B1V	+0.10	240
RR Sco	352.5	+ 7.8						+0.12	275
HD 152519	358.0	+13.0	6.72	+0.09	+0.07	2	A0	+0.10	100
152635	351.0	+ 7.5	7.68	-0.01	-0.41	C	B8	+0.15	360
152804	351.0	+ 7.5	8.70	+0.135	-0.265	2	B8	+0.28	465
153045	350.4	+ 6.5	9.13	+0.105	+0.01	2	B9	+0.15	350
θ Aps	307.2	-14.5							
HD 118285	305.9	-13.1	6.33	+0.01	-0.26	C	A0	+0.13	150
124639	305.9	-20.5	6.41	+0.02	-0.33	C	B8	+0.17	190
124771	306.9	-18.0	5.05	-0.11	-0.55	C	B3V	+0.08	140
131551	311.0	-14.2	6.19	-0.04	-0.19	C	B9	+0.05	125

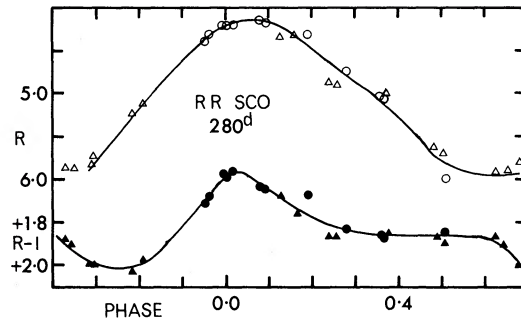
* See Wallerstein and Greenstein (1964, Figure 5).

FIG. 22.—Light and color curves (UBV) for RR Sco

with a modulus of 7.9 mag. The path traced in the (M_{bol} , $R - I$)-plane is shown by filled boxes in figure 24.

The light and color curves for θ Aps are shown in figure 27. The basic period is about 120 days. The star is a fundamental standard of the FK4 system, and the proper motion, with precessional corrections, is $(\mu_{\alpha}, \mu_{\delta}) = (-0.090, -0.033)$. The radial velocity is $+9.5 \text{ km s}^{-1}$. A value of $E(B - V) = +0.10 \text{ mag}$ is interpolated in the reddenings listed in table 2, giving $E(R - I) = +0.055 \text{ mag}$. Membership in the ζ Her Group gives $(U, V, W) = (+49, -47, -7) \text{ km s}^{-1}$ with a modulus of 5.85 mag. The variation is shown in the (M_{bol} , $R - I$)-plane of figure 24 by filled boxes.

The large-amplitude red variable R Leo is a member of the Wolf 630 Group. The observed cycles in 1972 and 1973 are shown in figures 28 and 29 by open circles and squares, respectively, and those observed in 1966 (Eggen 1967) and 1970 (Eggen 1971*b*, table 8) are shown as inverted and erect triangles, respectively. The phases are determined from the elements given in the GCVS; Max. = JD 2,437,339 + 312^d.56*E*. The period is similar to that of R Car, and the light curves

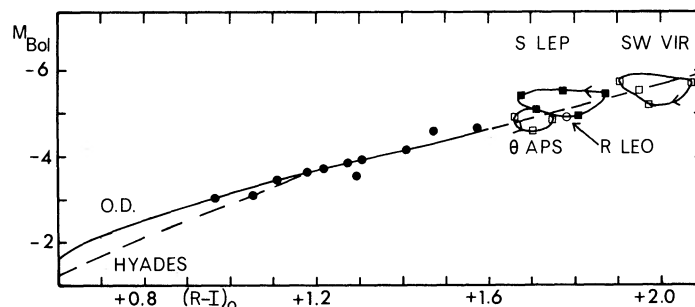
FIG. 23.—Same as fig. 22 but for (RI)

shown the same kind of variation between cycles as seen in figures 1 and 7. The star has a galactic latitude of $+44^\circ$, so possible reddening corrections will be ignored. The very well determined proper motion from meridian observations is $(\mu_{\alpha}, \mu_{\delta}) = (+0.005, -0.034)$ on the FK4 system with precessional corrections, and the probable error is 0.002. The radial velocity is $+13.4 \text{ km s}^{-1}$, and membership in the Wolf 630 Group gives $(U, V, W) = (-9, -33, +2) \text{ km s}^{-1}$ with a modulus of 6.4 mag. The position in the (M_{bol} , $R - I$)-plane for phase 0.2 in figure 29, or 0.25 from maximum light, which from the previous discussion should approximate closely the median magnitude and color, is shown by the open circle in figure 24.

The extension of the giant sequence shown as a broken curve for $R - I$ greater than $+1.6 \text{ mag}$ in figure 18 is repeated in figure 24, and obviously this represents as good a fit to the median luminosities of the old disk variables as can be derived from the present data. *The mean sequence for the Hyades and old disk variables—that is, the red giants with mass less than about three solar masses—can then be well represented by the relation $(M_{\text{bol}}(\text{Median})) = -0.65 \text{ mag} - 2.5(R - I)_0$.*

IV. LARGE-AMPLITUDE RED VARIABLES IN THE HALO POPULATION

The giant sequence derived from the cluster 47 Tucanae (Eggen 1972*a* and 1973*a*, table 9) is shown as a continuous curve in figure 30, which also contains the old disk and Hyades population sequences from figures 18 and 24. Two very small amplitude variables in 47

FIG. 24.—Old disk population variables in the (M_{bol} , $R - I$)-plane

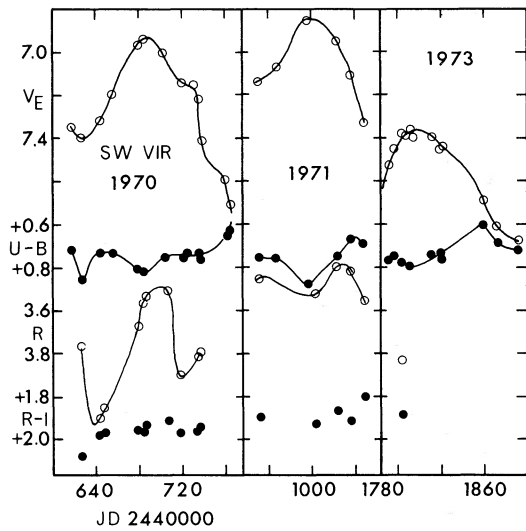


FIG. 25.—Light and color curves for SW Vir

Tucanae, Nos. 81 and 300 (Eggen 1972*a*, table 1), are shown as filled circles in figure 30. Variables Nos. 5 and 7 in this cluster are small-amplitude variables with visual range less than 0.5 mag and period near 50 days. Earlier observations published elsewhere (Eggen 1972*a*, table 15) are supplemented with the new results listed in the SUPP. The mean paths in the (M_{bol} , $R - I$)-plane are shown in figure 30 as filled squares.

Observations of two additional small-amplitude variables in 47 Tucanae, one of which is the known variable No. 11 and the other Wildey (1961) No. 12,

are also available. The new variable is shown in figure 31 and the observations of variable No. 11 are in figure 32. Variable No. 11 is identical with variable No. 5 shown in figure 30, and the new variable, Wildey 12, traces the path in the (M_{bol} , $R - I$)-plane of this figure as shown by the open squares. The position of Wildey 12 in figure 30 indicates that the giant sequences of disk and halo giants merge near $R - I = +1.2$ mag.

The cluster contains three large-amplitude variables with periods near 200 days. Observations of variable No. 3 (192^d) are shown in figures 33 and 34. The elements adopted here are Max. = JD 2,441,611 + 192.E. These elements give a maximum at JD 2,435,478 which agrees with JD 2,435,468 ± 10^d derived by Arp, Brueckel, and Lourens (1963). The range of $B - V$ found by Arp *et al.* is confirmed here, but their visual amplitude, derived from photographic plates, is 1 mag less. The new observations are shown as circles in figures 33 and 34 while the earlier observations (Eggen 1972*a*, table 15) are represented by squares. The variation in ($U - B$) is shown by crosses in figure 33. The mean magnitudes and colors are tabulated in table 1. The variation from cycle to cycle is apparently not as large as noted above for the old disk population stars. Also, the path traced in the (M_{bol} , $R - I$)-plane of figure 30 is strikingly different from the large loops shown by the old disk variables in this plane (e.g., fig. 18). The median values of V_E , R , and I , derived from the light curves in intensity units, are $\langle V \rangle = 11.67$ mag, $\langle R \rangle = 10.35$ mag, and $\langle I \rangle = 9.00$ mag. Unlike the old disk variables, where the median values correspond to those observed near

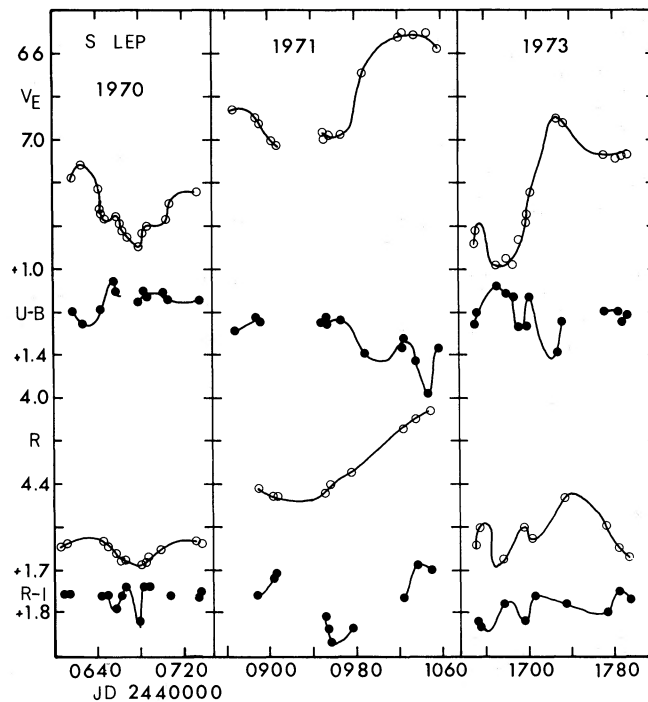


FIG. 26.—Light and color curves for S Lep

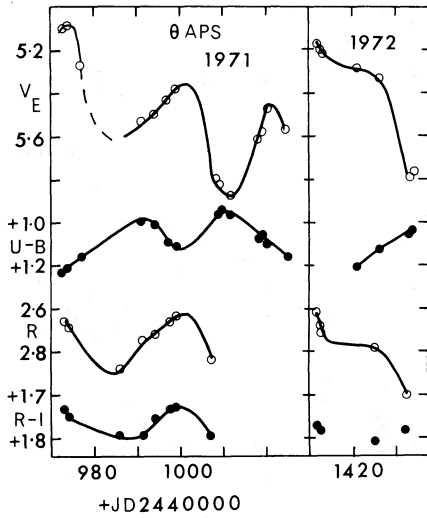


FIG. 27.—Light and color curves for θ Aps

quarter phase, those for variable No. 3 correspond to phase 0.2 for R and phase 0.11 for V_E . At quarter phase $(R - I)_0 = +1.52$ mag, $M_{bol} = -4.15$ mag, and this is indicated in figure 30 by an open square; the median values of $\langle R_0 \rangle - \langle I_0 \rangle = +1.33$ mag and $M_{bol} = -4.2$ mag are represented by the open circle. The linear approximation to the old disk population sequence, derived in the previous section, yields $M_{bol} = -4.0$ mag, and it is uncertain if the small residual of -0.2

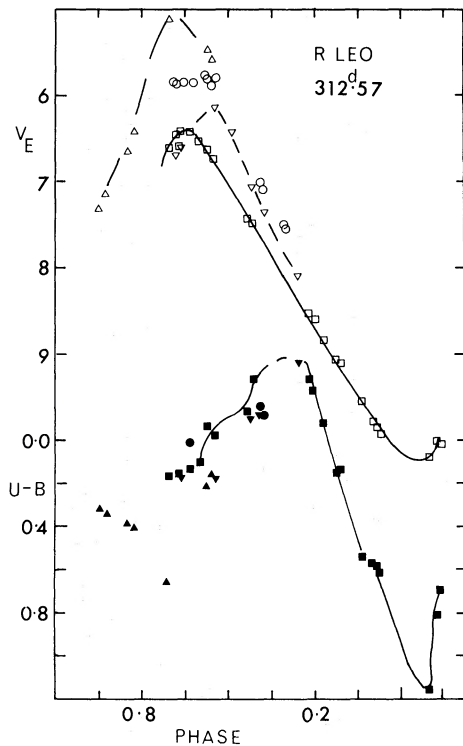


FIG. 28.—Light and color curves (UBV) for R Leo

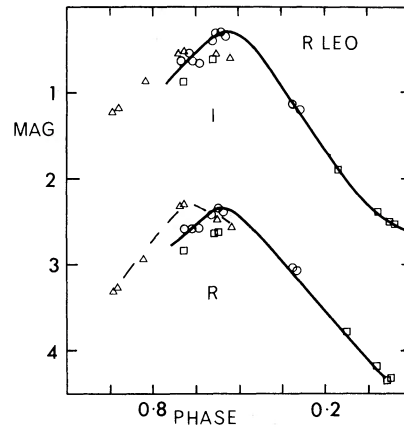


FIG. 29.—Same as fig. 28 but for (RI)

mag found from the median values results from small errors in the definition of the light curves, from which the median values are obtained, or from a real

TABLE 3

LARGE AMPLITUDE VARIABLES

I*	II	III	IV	V	VI	VII
RU Vir 436.52 34742	+ 1.42 - 4.1 11.3	+ 4 -35 + 2.0	-180 -215 -115	- 99 -118 - 64	-197 -337 +920	SN 0.00 Mc
R Oct 405.0 41170	+ 1.87 - 5.3 10.0	+ 4 +39 +46.0	+147 -112 - 48	+167 - 77 - 26	-428 -769 -476	Me 0.00 C
RR Sgr 334.4 41130	+ 1.80 - 5.15 7.4	-20 -27 +85.0	- 90 - 28 - 24	- 52 -144 + 45	-880 +184 -438	Me 0.00 M
R Car 310.0 41060	+ 1.75 - 5.0 7.1	-28 + 9 +28.1	+ 27 - 32 - 19	+125 - 19 - 59	-210 -967 -143	Me +0.04 M
T Col 225.5 37885	+ 1.66 - 4.8 9.8	+24 +19 +97.0	+113 - 71 + 64	+ 91 - 26 +110	+455 -706 -543	Me 0.00 M
T Hor 217.0 41530	+ 1.75 - 5.0 11.75	+21 +10 +50.0	+216 -124 + 34	+ 96 - 43 + 34	+ 44 -557 -829	Me 0.00 Mc
R Vir 148.0 41038	+ 1.61 - 4.7 9.65	-36 + 9 -25.0	+145 - 39 - 18	+167 - 55 + 6	-140 -319 +937	Me 0.00 M
T Gru 136.6 40446	+ 1.15 - 3.5 10.95	- - +14.0	- - -	- - -	-532 + 45 -846	Me 0.00 -
R Vul 136.8 41615	+ 1.49 - 4.4 10.6	+ 4 + 2 -12.0	+ 30 - 5 - 8	+ 19 + 4 - 8	-322 +910 -262	Me +0.08 Mc,M
W Pup 120 41245	+ 1.42 - 4.2 10.6	+15 + 3 +17.0	- 21 - 36 + 87	- 19 - 15 + 68	+236 -960 -151	Me +0.15 Mc,Y,C

* The periods and epochs of maxima for R Car, T Hor and R Vir, although not used in the present discussion, are based on the new observations. The periods for the other stars are from the GCVS but in some cases new epochs have been determined from the present data.

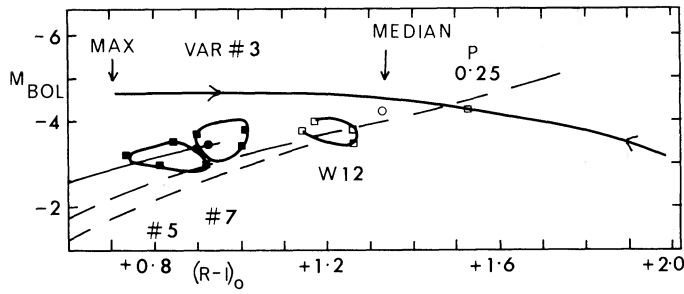


FIG. 30.—Halo population variables in the (M_{bol} , $R - I$)-plane

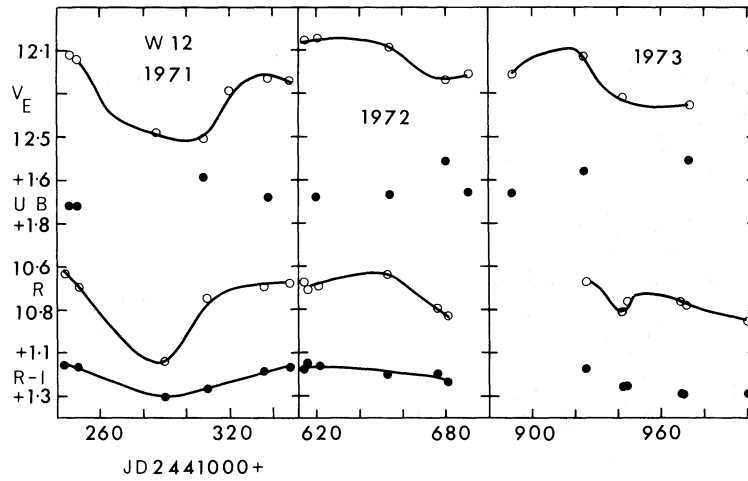


FIG. 31.—Light and color curves for a new variable, Wildey No. 12, in 47 Tuc

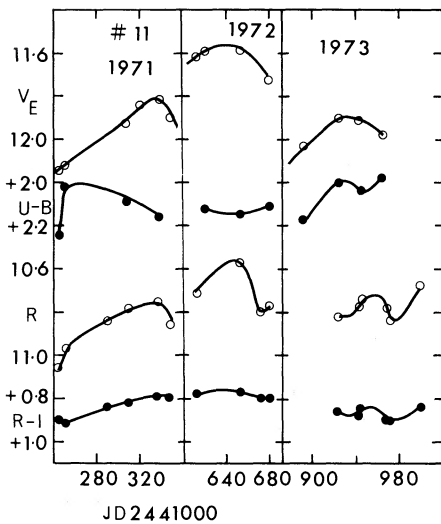


FIG. 32.—Light and color curves for variable No. 11 in 47 Tuc.

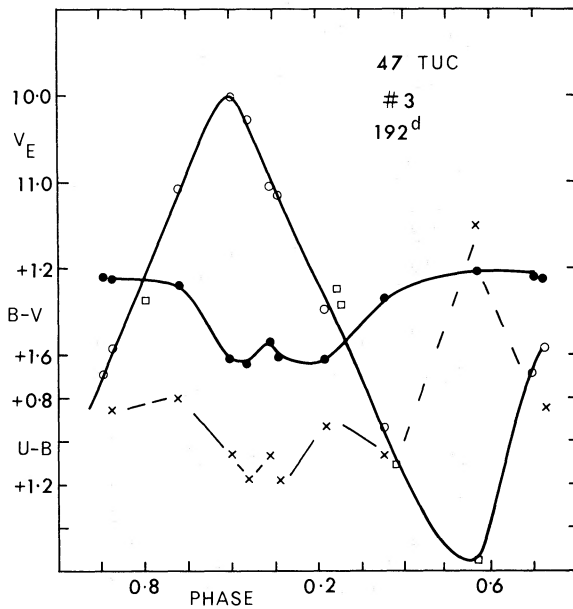
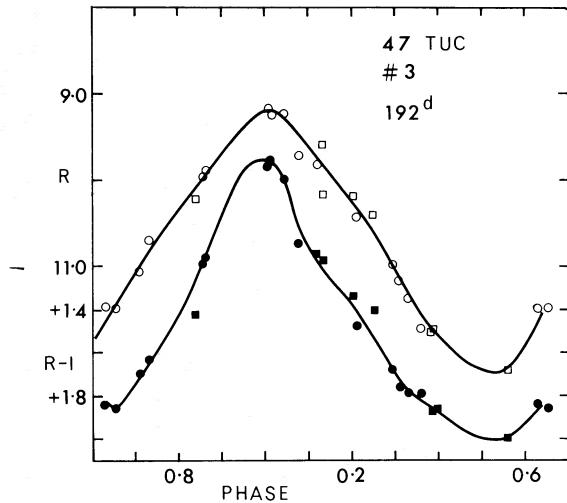


FIG. 33.—Light and color (UBV) curves for variable No. 3 in 47 Tuc.

FIG. 34.—Same as fig. 33 but for (RI)

luminosity difference in the giant sequences of the two populations at $R - I$ near +1.4 mag.

V. DISCUSSION

a) Luminosities

By using small and intermediate amplitude variables, for which accurate median parameters can be obtained, to extend the giant sequence defined by constant stars in the old disk population (i.e., stars with mass near $3 M_{\odot}$ or less) to lower temperatures, it is found that the luminosities of large-amplitude variables in the groups and clusters containing old disk and halo populations can be predicted with accuracy, and a convenient luminosity to adopt for these variables is that near quarter phase after maximum light. The giant sequence is closely approximated by the relation $M_{\text{bol}} = -0.65 \text{ mag} - 2.5(R - I)_0$.

This approximation has been applied to the stars discussed in § I and listed in table 3, which contains the following information: Column (I), Name/period/epoch of maximum less JD 2,400,000. Column (II), $(R - I)_0$ at phase $0.25/M_{\text{bol}}/\text{modulus}$. Column (III), $(\mu_{\alpha}/\mu_{\delta})/(0.001)/\text{radial velocity (km s}^{-1}\text{)}$. Column (IV), $U/V/W$ (km s $^{-1}$). Column (V), $dU/dV/dW$ for a 1000-pc increase in distance. Column (VI), direction cosines. Column (VII), Sp. type/ $E(R - I)$ /Source of proper motion; M = Meridian, C = Cape Zone catalogs, Y = Yale Zone catalogs, and Mc = photographic determinations by Alden and Osvalds (1961).

All proper motions are on the FK4 system with precessional corrections. The values of $E(B - V)$ are derived from the values of $E'(B - V)$ interpolated in the reddening determinations from B-type stars in the vicinity of these variables; the remaining stars are at high galactic latitudes, and the possible reddening has been ignored.

RU Virginis is a carbon star (R3) but is redder than other R0-R5 objects which have values of $R - I$ in the range 0.3-0.6 mag (Eggen 1972c). However, it is

similar in both color and motion to the variable TT CVn (Eggen 1969a, table 1), a CH star. The latter variable is 1000 pc above the galactic plane and has W near -100 km s^{-1} compared with RU Vir which is 1700 pc above the plane with $W = -115 \text{ km s}^{-1}$. Photometrically and kinematically RU Vir also bears some resemblance to the SN star FU Mon (Eggen 1972b, table 17).

The proper motion of R Vir is very well determined from meridian observations and has a probable error of 0.002 . This motion agrees with that derived by Alden and Osvalds (1961) and from the Toulouse astrophotographic plates (Paloque, Pretre, and Reynis 1969):

$$\text{Meridian: } \mu_{\alpha} = -0.036, \quad \mu_{\delta} = +0.009;$$

$$\text{Mc: } \mu_{\alpha} = -0.035, \quad \mu_{\delta} = +0.008;$$

$$\text{Toulouse: } \mu_{\alpha} = -0.035, \quad \mu_{\delta} = +0.009.$$

However, the same cannot be said for the motion of T Gru for which only photographic determinations are available:

$$\text{Y: } \mu_{\alpha} = -0.012, \quad \mu_{\delta} = +0.005;$$

$$\text{C: } \mu_{\alpha} = -0.053, \quad \mu_{\delta} = -0.002;$$

$$\text{Mc: } \mu_{\alpha} = +0.005, \quad \mu_{\delta} = -0.0031$$

In view of the large uncertainty, no space motion is given for this object in table 3. The McCormick photographic result and the motion obtained from the meridian observations are identical for R Vul. The Yale and Cape photographic zones also give identical proper motions for W Pup, but the McCormick value is larger:

$$\text{Y, C: } \mu_{\alpha} = +0.003, \quad \mu_{\delta} = +0.004;$$

$$\text{Mc: } \mu_{\alpha} = +0.023, \quad \mu_{\delta} = +0.002,$$

and a mean of $(+0.015, +0.003)$ has been adopted. The motions of the other stars are taken from the sources indicated in table 3.

The mean luminosity of a small amplitude variable of type S, π^1 Gru in the Hyades Group, is $M_{\text{bol}} = -4.9 \text{ mag}$ (§ III), and the same value is computed from the median value of $(R - I)_0 = +1.70 \text{ mag}$. However, some attention must be paid to the band-passes of the filters used in the (RI) photometry in the case of such complicated spectra as those presented in the red by the S-type stars. Although, as noted above, the filter combinations used by Mendoza (1967) and Barnes (1974) give results for the M-type variables that can be transformed to the system used here, this may not be the case for the S-type stars. For example, a series of observations of π^1 Gru near minimum light by Mendoza (1967) gives $(R - I)_J = +2.64 \text{ mag}$ or $(R - I) = 0.80(R - I)_J - 0.05 \text{ mag} = +2.06 \text{ mag}$, which is considerably redder than the value of +1.8 mag observed here at minimum light. Therefore, confirmation of the applicability of the calibration

derived above for the luminosities of the large-amplitude variables of type S must await the availability of observations, on the present system, of such group members as R And, spectral type S, of the Wolf 630 Group (Eggen 1972*b*, table 1). However, the median colors of the small amplitude variables and the apparently nonvariable S-type stars, such as HD 34738, 35155, 49365, 58881, 63773, 64332, and 216672, yield the same luminosity from the present calibration as was obtained in an earlier discussion (Eggen 1972*b*, table 1). The same situation obtains for the MS stars (Eggen 1972*b*, table 5) and the very small amplitude, very short period variable HR 1566, spectral type M3S, which is a member of the Wolf 630 Group, has a median value of $(R - I)_0 = +1.13$ mag (Eggen 1973*b*), giving a computed value of $M_{\text{bol}} = -3.5$ mag, compared with -3.6 mag obtained from the group motion (Eggen 1971*b*, table 3).

The combination of (RI) observations of N-type stars made in different photometric systems might also be suspect. However, apparently those obtained in the $(RI)_J$ system can be reduced to the system used here with the transformation equations derived from late-type, nonvariable stars (Eggen 1971*d*). For example, the small-amplitude variable HD 75021, of type N, has mean values of $(R, R - I) = (6.05 \text{ mag}, +0.96 \text{ mag})$ (Eggen 1972*b*, table 10) while the results given by Mendoza and Johnson (1965) convert to $(6.00 \text{ mag}, +0.99 \text{ mag})$. Also, the intermediate-amplitude variable U Hya has

$$(V_B, B - V, R, R - I) \\ = (4.80, +2.42, 3.43, +0.93 \text{ mag})$$

near median light whereas observations by Mendoza (1967) give $(4.70, +2.50, 3.40, +0.93 \text{ mag})$. The calibration of luminosities derived here can be tested for the N-type stars with the carbon star found by Catchpole and Feast (1973) to be a member of NGC 2477. Recent observations have shown this object to be a small-amplitude variable with median values of $(R, R - I) = (8.5 \text{ mag}, +1.28 \text{ mag})$. The star, and the cluster, will be discussed in more detail elsewhere; but adopting the mean reddening $E(B - V)$, and distance, $V_0 - M_v$, obtained by Hartwick, Hesser, and McClure (1972), of $+0.30 \text{ mag}$ and 10.6 mag , respectively, we have $M_{\text{bol}} = -3.5$ at $(R - I)_0 = +1.07 \text{ mag}$, whereas the luminosity calibration derived above would predict -3.3 mag .

b) Period-Luminosity Relation

It was shown elsewhere (Eggen 1973*c*) that the periods and colors of small-amplitude red variables are not related. However, the relation $M_{\text{bol}} = -0.65 - 2.5 \text{ mag } (R - I)_0$, in addition to the fact that, as discussed above, the large-amplitude variables populate the giant sequence in the $(M_{\text{bol}}, R - I)$ -plane, leads to the presence of a period luminosity relation if the periods and colors, at median light or phase 0.25, are related. The stars in table 3 are shown in the $(\log P, R - I)$ -plane of figure 35 as open circles. The

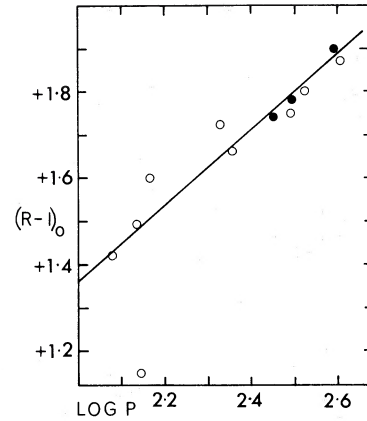


FIG. 35.—The correlation between median color for large-amplitude variables in the field (*open circles*), and groups (*filled circles*).

values of $(R - I)_0$ in table 3, read at phase 0.25, are used. Also, the two large amplitude variables in the Hyades Group (§ III*a*) and the one in the Wolf 630 Group (§ III*b*) are shown in figure 35 as filled circles. The halo population star, variable No. 3 in 47 Tucanae, and the carbon variable RU Vir in table 3 are omitted so as to restrict the objects discussed here to the old disk population, M-type stars. The deviant star in figure 35, indicated by an open circle at $R - I = +1.15 \text{ mag}$, is T Gru for which no space motion is given in table 3 because the proper-motion determinations, discussed above (§ V*a*), are very discordant. However, if either of the two largest proper motions published for this star are correct, it is a halo population object and, as discussed below, its position in figure 35 is understandable for that reason. Several additional stars, covering the period range of 120–500 days but not discussed here, confirm the relation in figure 35. The linear relation in the figure is given by $(R - I)_0 = -0.45 \text{ mag} + 0.90 \log P$ which, when combined with the color luminosity relation, gives

$$M_{\text{bol}} = +0.5 \text{ mag} - 2.25 \log P.$$

The bolometric luminosities discussed here have been derived on the basis that $M_{\text{bol}} = M(I)_J + 1 \text{ mag} = M(I) - 0.25(R - I) + 0.56 \text{ mag}$. This follows from the fact, noted elsewhere (Eggen 1971*a*, table 5), that values of $-(V - I)_J + 1 \text{ mag}$ taken from a tabulation of mean values of $(V - I)_J$ at various spectral types and luminosities (Johnson 1966) represent, within 0.1 mag, the bolometric corrections derived by Johnson from *IJKLMN* photometry with careful consideration given to bands of H_2O and other marked spectral features. These bolometric corrections are shown in the $(B.C., R - I)$ -plane of figure 36 as filled circles, and the linear relation is represented by

$$B.C. = +0.60 \text{ mag} - 2.5(R - I).$$

The bolometric corrections for the reddest stars are confirmed by some independent determinations derived

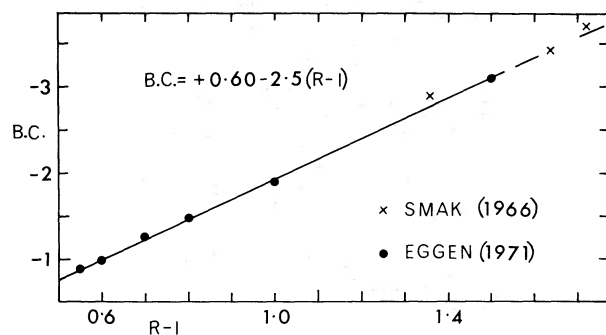


FIG. 36.—Correlation between the bolometric corrections and the $(R - I)$ color.

by Smak (1966) and shown in figure 36 as crosses. It perhaps is not surprising that I magnitudes should approximate bolometric magnitudes over the temperature range considered here because, with an effective wavelength near 1μ , these magnitudes refer to a spectral region near the energy peak of these stars. Earlier derivations of bolometric corrections (e.g., Smak 1964), which were based on blackbody considerations, required knowledge of the TiO blanketing, and estimates of this blanketing in V at, say,

$$M_5(R - I) = +1.50 \text{ mag},$$

ranged from 0.6 mag (Kubiak 1966) to 1.6 mag (Smak 1964) with a consequential uncertainty in the derived corrections.

The combination of the relations derived above gives

$$\begin{aligned} M_V(\text{Median}) &= M_{\text{bol}}(\text{Median}) - \text{B.C.} \\ &= -1.25 \text{ mag}, \end{aligned}$$

and over the period and temperature range discussed here all of the large-amplitude red variables have the same median visual luminosity. The variables all have $B - V$ near +1.5 mag, so $M_B = +0.25$ mag.

The belief that a relation exists between M_V and period, and that this relation has a slope near 4 or 5 $\log P$ with the longest periods having the lowest luminosity, has existed for 50 years and is based entirely on statistical parallax results for these objects. The early studies are summarized by Wilson and Merrill (1942) and Osvalds and Risley (1961). More recently Clayton and Feast (1960) have reexamined the question and have found that at mean light intensity, which should correspond closely to the intensity at phase 0.25 as described above, $M_V = -1.5$ mag for stars with periods between 150 and 200 days. However, they also found that M_V is only -0.5 mag for stars with periods between 200 and 250 days and, within the uncertainty of the data, near $+0.5$ mag for those with periods from 300 to 450 days. One consequence of this rapid decline in luminosity with increasing period is that, although the kinematics of stars with periods shorter than 300 days yield values of the Oort constant A that are very similar to those obtained for the

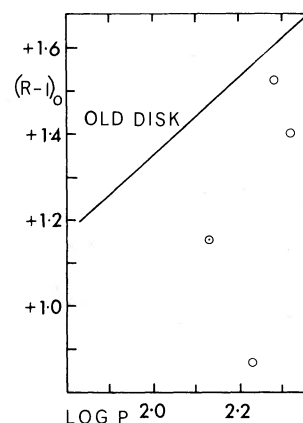


FIG. 37.—The halo variables in the $(R - I, \log P)$ -plane

Cepheid variables, the longer period stars yielded values twice as large (Smak and Preston 1965). Although there are several difficulties in the interpretation of these results as noted by Smak and Preston (see also Feast 1972), the simplest explanation is that the distances of the longer period stars were overestimated by the use of a period-luminosity relation. Smak and Preston used a relation with a slope of $5.4 \log P$, making a 500-day variable 1.5 mag fainter than a 250-day variable, and the resulting differential in distance would produce the observed effect on A .

It is of course probable that for stars with periods longer than 500 days, and therefore redder than $R - I = +1.8$ mag at median light, the relation between $R - I$ and the bolometric correction will become non-linear, with a large increase in the bolometric correction for small changes in $R - I$. For these stars, which are few in number, the bolometric corrections may overcompensate for the slope of the period (bolometric) luminosity relation, giving lower (visual) luminosities than $M_V = -1.2$ mag.

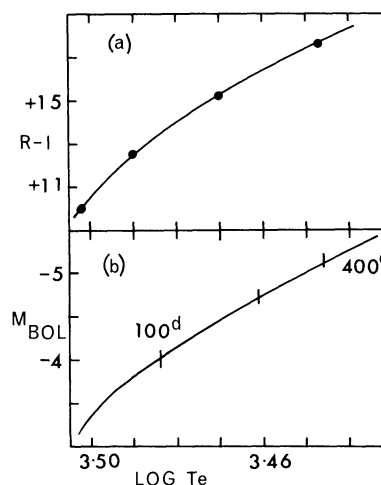


FIG. 38.—(a) the $(R - I, \log T_e)$ and (b) $(M_{\text{bol}}, \log T_e)$ relations. The median luminosity of large amplitude variables of various periods are marked in fig. 38b.

In contrast with the old disk population stars, the halo variables shown in the $(R - I, \log P)$ -plane of figure 37 indicate little or no correlation between period and the color read at phase 0.25. In addition to T Gru, the deviant star in figure 35, and Variable No. 3 in 47 Tucanae, discussed above, figure 37 contains R Pic ($P = 170^d$; Eggen 1972a, table 26) and T Scl ($P = 212^d$; Eggen 1970). Large-amplitude red variables of the halo population are rare, although the intermediate-amplitude objects of this population, such as S Car and L² Pup, which will be discussed elsewhere, are well represented among the brightest variables. The wide range of colors represented in figure 37, indicating the

lack of a period-color relation, allows nothing to be said concerning a period-luminosity relation, although the color-luminosity relation, on the basis of the variables in 47 Tucanae, appears to be the same as for the old disk stars.

The calibration of the $(R - I, \log T_e)$ -relation given by Johnson (1966) is shown in the top panel of figure 38. Applying this calibration to the giant sequence of the red variables gives the $(M_{\text{bol}}, \log T_e)$ -relation shown in the bottom panel of the figure. The median luminosities of large amplitude red variables of various periods are also indicated.

REFERENCES

- Alden, A. L., and Osvalds, V. 1961, *Pub. Leander McCormick Obs.*, Vol. **11**, Part 20.
- Arp, H. C., Brueckel, F., and Lourens, J. V. B. 1963, *Ap. J.*, **137**, 228.
- Barnes, T. G., III. 1974, *Ap. J. Suppl.*, **25**, 369 (No. 221).
- Blackwell, K. C., and Lowne, C. M. 1968, *R.O.B.*, No. 142.
- Catchpole, R. M., and Feast, M. W. 1973, *M.N.R.A.S.*, **164**, 111.
- Clayton, M. L., and Feast, M. W. 1969, *M.N.R.A.S.*, **146**, 411.
- Eggen, O. J. 1967, *Ap. J. Suppl.*, **14**, 307 (No. 131).
- . 1969a, *Pub. A.S.P.*, **81**, 346.
- . 1969b, *Ap. J.*, **158**, 225.
- . 1970, *Ap. J. Suppl.*, **22**, 289 (No. 188).
- . 1971a, *Ap. J.*, **163**, 313.
- . 1971b, *ibid.*, **165**, 317.
- . 1971c, *Pub. A.S.P.*, **83**, 251.
- . 1971d, *Ap. J. Suppl.*, **22**, 389 (No. 191).
- . 1972a, *Ap. J.*, **172**, 639.
- . 1972b, *ibid.*, **177**, 489.
- . 1972c, *M.N.R.A.S.*, **159**, 403.
- . 1972d, *Pub. A.S.P.*, **84**, 406.
- . 1973a, *Pub. A.S.P.*, **85**, 542.
- . 1973b, *Ap. J.*, **180**, 857.
- Eggen, O. J., 1973c, *ibid.*, **174**, 793.
- . 1974a, *Pub. A.S.P.* (in press).
- . 1974b, *Ap. J. Suppl.* (in press).
- Feast, M. W. 1972, *Vistas in Astronomy*, **13**, 207.
- Fernie, J. D. 1963, *A.J.*, **68**, 780.
- Hartwick, F. D. A., Hesser, J. E., and McClure, R. D. 1972, *Ap. J.*, **174**, 557.
- Hoffleit, D. 1967, *Trans. Yale Obs.*, p. 29.
- Johnson, H. L. 1966, *Ann. Rev. Astr. and Ap.*, **4**, 193.
- Kubiak, M. 1966, *Acta Astr.*, **16**, 275.
- Lockwood, G. W., and Wing, R. F. 1971, *Ap. J.*, **169**, 63.
- Mendoza, E. E. 1967, *Bol. Obs. Tonantzintla y Tacubaya*, **4**, 114.
- Mendoza, E. E., and Johnson, H. L. 1965, *Ap. J.*, **141**, 161.
- Osvalds, V., and Risley, A. M. 1961, *Pub. Leander McCormick Obs.*, Vol. **11**, Part 21.
- Paloque, E., Pretre, P., and Reynis, M. 1969, *Ann. Obs. Toulouse*, **27**, 7.
- Smak, J. 1964, *Ap. J. Suppl.*, **9**, 141 (No. 89).
- . 1966, *Acta Astr.*, **16**, 1.
- Smak, J., and Preston, G. W. 1965, *Ap. J.*, **142**, 943.
- Wallerstein, G., and Greenstein, J. L. 1964, *Ap. J.*, **139**, 1163.
- Willey, R. L. 1961, *Ap. J.*, **133**, 430.
- Wilson, R., and Merrill, P. 1942, *Ap. J.*, **95**, 265.

O. J. EGGEN: Mount Stromlo and Siding Spring Observatory, Private Bag, P.O. Woden, A.C.T., Australia 2606